Reprinted from the *Soil Science Society of America Journal*
Volume 41, no. 1, January-February 1977
677 South Segoe Rd., Madison, WI 53711 USA

Gully Wall Stability in Loess-derived Alluvium[1]

J. M. BRADFORD AND R. F. PIEST[2]

ABSTRACT

A field study was made on an instrumented vertical slope to investigate the triggering mechanisms that initiate gully wall failure in loess-derived alluvium. The relevance of hydrology, soil morphology, and soil mechanics to an understanding of gully slumping is examined. Conventional limit equilibrium slope stability methods were of little value in predicting failure volumes or in understanding the failure mechanics. The geometry and time of failure are greatly influenced by the structural features of loess-derived alluvium and by the dependence of the shear strength on the pore water pressure within the soil.

Additional Index Words: **soil mechanics, soil strength, soil morphology, erosion, sedimentation, slope stability, ground water.**

IN THE THICK LOESSIAL AREAS of the world, gully erosion contributes greatly to the pollution of water bodies and to loss of valuable lands for crop production. In the Missouri River Basin, near-vertical walls exist around the head-scarp perimeter of valley-bottom gullies, after each succession of fallen debris has been removed by runoff. The failure of these near-vertical walls is the initiation of continued upstream advance. Downstream from the head scarp, the widening of gullies due to bank slumping contributes in a lesser degree to the total gully sediment yield. The depth and velocity of the flowing water is insufficient to remove material accumulated from bank slumping (Brice, 1966).

The development of gully walls is influenced by many factors and thus cannot be fully evaluated. Failure occurs when the driving forces of the soil mass equal or exceed the resisting forces. Gully slopes are loaded by three different categories of forces: (i) weight of the soil mass, (ii) weight of water added to the soil mass either by surface infiltration or rise in water table, and (iii) seepage forces of percolating water. Forces that resist failure are due to the shear strength of the soil mass. As water content increases, shearing resistance decreases. The in situ shear strength is also influenced by freezing and thawing and wetting and drying cycles.

[1]Contribution from the North Central Region, ARS, USDA in cooperation with the Missouri Agric. Exp. Stn., Columbia, Missouri. J. Ser. no. 7452. Received 19 April 1976. Approved 20 Sept. 1976.

[2]Soil Scientist, USDA-ARS and Dep. of Agronomy, Univ. of Missouri; Hydraulic Engineer, USDA-ARS, respectively. Both are in Columbia, MO 65201.

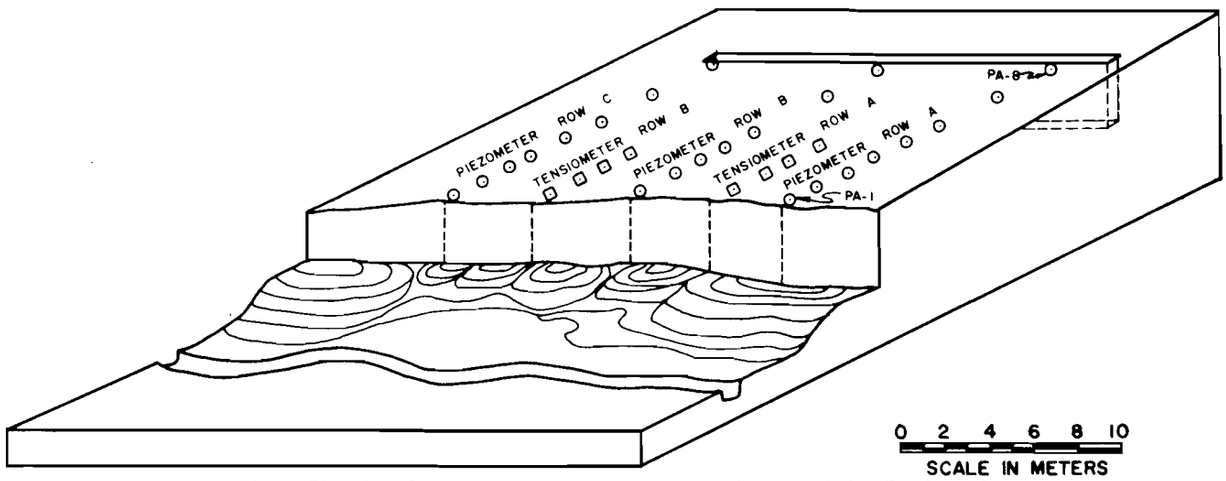

Fig. 1—Plan view of tensiometers and piezometers in relation to vertical wall and trench.

Vertical tension cracks at the surface of the slope, possibly occurring along natural cleavage planes, reduce the overall stability of a slope by decreasing the cohesion which can be mobilized along the upper part of a potential failure surface. Water infiltration from the soil surface into the cracks also increases the pore water pressures acting on the failure surface. Defining a factor of safety against failure is difficult due to the many parameters involved.

Much of our knowledge regarding gully wall failures has been obtained from passing observations without regard to detailed analyses of conditions causing failure. For example, engineers on storm duty (collecting sediment samples) at the Treynor, Iowa, ARS watersheds reported that undercutting at the toe of the slope nearly always preceeds massive slope slumping. Some think the V- and U-shaped gullies in the loessial areas of Missouri are a result of different patterns of freezing and thawing. Intensive gullying in western Iowa during May and June has been explained on the basis of high-water tables during early spring. This investigation made full-scale tests (2-dimensional) in the field with controlled groundwater conditions and attempted to relate failure conditions and patterns of vertical walls with past observations from gully erosion studies.

Site Geometry and Instrumentation

The site for the study was watershed 3 near Treynor, Iowa, in Pottawattamie County. Watersheds and gullies are described by Saxton and Spomer (1968), Piest and Spomer (1968), and Piest et al. (1975).

The field study was designed to control the water table within the soil mass and to observe failure as a function of pore water pressure. Along an 18-m length of gully channel, about 120 m downstream from the gully headcut, a clean, vertical wall was formed by cutting about 3 m back into the existing wall. The height from the toe of the gully bank to the surface varied from 3.5 m at the southern end to 2.8 m at the northern end. A trench was cut parallel with the vertical wall, 14.4 m from the wall, to a depth of 3.0 m to control the water table within the soil area between the vertical wall and the trench. A floating device, attached to an electric water pump system, was placed in the trench for controlling the water level within the trench. Clear water was obtained from a pool downstream.

A network of tensiometers to measure the negative pore water pressures and piezometers to measure positive pore water pressures was placed within the area, as shown in Fig. 1. The piezometer sets were placed in three rows perpendicular to the vertical gully wall—one row in the center part and two about 3 m from each end. Eight sets of six piezometers were installed to 2.0, 2.6, 3.2, 4.1, 4.7, and 5.3 m depths at eight locations as shown in Fig. 1. The piezometers were of 1.27 cm diameter pipe pushed into the ground by an Acker[3] hydraulic sampler. A plug was inserted into the lower end of the pipe for installation and then forced out at the desired depth. Then the piezometer tube was flushed by sucking water through the pipe with a vacuum pump. Each pipe was flushed and tested for response.

Four sets of the Lark[3] mercury manometer type tensiometers were installed to 1.2, 1.5, 1.8, 2.1, and 2.4 m depths in each of two rows (Fig. 1) perpendicular to the vertical gully wall.

There was a thick bromegrass *(Bromus inermis)* cover on the land surface which was kept mowed during the experiment.

Geology and Morphology

The test site is situated on loess-derived alluvium which has strata that can be related to the Pleistocene history of the region, characterized by Daniels and Jordan (1966) and Ruhe, et al. (1967). The Pleistocene and Recent deposits in the Treynor, Iowa, watershed 3 are described in detail by W. H. Allen[4] (1971).

The study area has been subjected to two major glaciations, the Nebraskan and the Kansan; each was followed by soil-forming periods, erosion, and landscape formation. The till deposits and landscapes were subsequently overlain by two major loess sheets—Loveland loess, which is Illi-

[3] Trade names and company names, included for the benefit of the reader, do not imply endorsement or preferential treatment of the product listed by the USDA.

[4] W. H. Allen, Jr. 1971. Landscape evolution and soil formation Treynor, Iowa. Ph.D. Thesis. Iowa State Univ., Ames.

noian in age, and Wisconsinan loess. Wisconsinan loess deposition began about 25,000 years ago and continued to about 14,000 years ago (Ruhe, et al., 1967). After loess deposition, erosion removed materials from hillsides and valley floors; the resulting deposition is herein described as loess-derived alluvium.

The post-Wisconsin alluvium was deposited from 14,000 to about 88 years before present, and has been defined by Daniels and Jordon (1966) and described by W. H. Allen[4] (1971) as the DeForest formation. The members of the DeForest formation (listed from the lowest) are Soetmelk, Watkins, Hatcher, Mullenix, and Turton. Allen[4] (1971) identified each member within the study area, except for the Soetmelk member. However, he states that its areal distribution is sporadic.

The morphology of the soil at the study site, as described by Charles Fisher[5], Soil Conservation Service, follows:

Horizon	*Depth*	*Description*
All	0-23 cm	Black (10YR 2/1) light silty clay loam; moderate fine granular and very fine subangular blocky structure; friable; common roots; clear smooth boundary.
A12	23-47 cm	Black (10YR 2/1) silty clay loam; strong angular and subangular blocky structure; friable; some oxidized organic material in old root channels—apparently tree roots; common grass roots; gradual smooth boundary.
A13	47-66 cm	Black (10YR 2/1) silty clay loam; moderate medium prismatic structure parts to moderate fine and medium subangular blocky; mainly friable but some peds are firm; common grass roots; common fine brown (7.5 YR 4/4) oxide stains and fine accumulations of oxides which are especially evident on cut faces of peds, apparent oxidation or organic material in grass or other root channels; gradual smooth boundary.
A3	66-94 cm	Very dark gray (10YR 3/1) light silty clay loam; weak medium prismatic structure parts to weak fine and medium subangular blocky; friable; common grass roots; common oxide stains and accumulations similar to the horizon above; gradual smooth boundary.
Bg	94-124 cm	Dark gray (10YR 4/1) light silty clay loam; common dark grayish brown (2.5Y 4/2) mottles which increase in number with depth; weak medium subangular blocky structure with some vertical cleavage; friable; 10 cm zone at top of horizon with evident accumulation of oxides in old root channels—colors are strong brown (7.5 YR 5/6) and reddish brown (5YR 4/4); gradual smooth boundary.
C1g	124-155 cm	Dark grayish brown (2.5Y 4/2) heavy silt loam; some dark gray (10YR 4/1) on faces of vertical cleavage planes; few grayish brown (2.5Y 5/2) to light olive brown (2.5Y 5/4) mottles in the lower part; very weak medium subangular blocky structure with some vertical cleavage that is weaker than in the horizon above; friable; few brown (7.5YR 4/4) oxide accumulations in old root channels; few roots; gradual smooth boundary.
C2g	155-200 cm	Grayish brown (2.5Y 5/2) silt loam; common light olive brown (2.5Y 5/4) mottles; massive but with some evidence of weak vertical cleavage; friable; some fine brown (7.5YR 4/4) oxide accumulations in old root channels; gradual smooth boundary.
C3g	200-254 cm	Grayish brown (2.5Y 5/2) silt loam;

[5]Charles S. Fisher, Assistant State Soil Scientist, Soil Conservation Services, Des Moines, Iowa, personal communication.

Table 1—Soil properties at Treynor, Iowa, Watershed 3, gully study area.

Member of De Forest formation	Depth	Sand (2-0.05 mm)	Silt (0.05-0.02 mm)	Silt (0.02-0.002 mm)	Clay (<0.002 mm)	Organic matter	pHw†	pHs‡
	cm			%				
Turton	0-15	4	34	31	31	3.7	6.8	6.0
	15-31	4	33	32	31	4.4	6.8	5.9
	31-46	4	31	32	33	2.7	7.0	6.0
	46-61	5	32	32	31	1.5	7.1	6.1
	61-76	5	35	29	31	1.6	7.2	6.2
	76-91	5	35	28	32	1.4	7.2	6.3
	91-107	4	36	29	31	1.1	7.4	6.5
	107-122	4	37	29	30	1.3	7.5	6.7
	122-137	5	37	28	30	1.2	7.5	6.7
	137-152	5	38	28	29	0.9	7.4	6.7
	152-168	5	37	28	30	0.9	7.7	6.6
	168-183	5	37	29	29	0.8	7.7	6.7
	183-198	5	37	29	29	0.9	7.6	6.6
	198-213	5	38	29	28	0.7	7.5	6.7
	213-229	5	38	29	28	0.8	7.8	6.8
	229-244	5	38	28	29	0.7	7.5	6.7
	244-259	5	38	28	29	0.8	7.8	6.9
	259-274	4	39	29	28	0.7	7.7	6.6
	274-290	4	39	29	28	0.8	7.7	6.6
	290-305	6	37	28	29	0.7	7.6	6.8
	305-320	6	37	28	29	0.7	7.7	6.9
	320-335	6	37	29	28	0.7	7.8	6.9
Mullenix	335-366	5	34	31	30	0.7	7.8	7.3
	366-396	3	37	30	30	0.7	8.0	7.4
	396-427	3	38	32	27	0.6	8.1	7.3
	427-457	3	40	30	27	0.7	8.1	7.4
Hatcher	457-488	4	37	31	28	1.1	8.1	7.2
	488-518	3	40	31	26	0.8	7.9	7.3
	518-549	3	38	30	29	1.0	8.1	7.2
	549-579	4	40	30	26	1.3	8.0	7.3
	579-610	3	38	31	28	1.1	8.0	7.1
	610-640	4	41	30	25	1.0	7.9	7.2
	640-671	5	41	29	25	0.7	7.8	7.1
	671-701	3	45	29	23	0.7	7.9	7.3
	701-732	5	43	30	22	1.0	8.1	7.3
	732-762	5	44	29	22	1.2	8.1	7.2
	762-792	4	42	30	24	1.0	8.1	7.3
	792-823	4	43	29	24	0.8	8.0	7.2
	823-853	3	42	29	26	1.3	8.2	7.3
Watkins	853-884	2	40	33	25	1.9	7.7	7.2
	884-914	3	39	32	26	2.4	7.9	7.3
	914-945	3	39	34	24	3.0	7.7	7.2
	945-975	3	36	36	25	3.0	7.8	7.2
	975-1006	5	39	31	25	3.0	7.7	7.2
Kansan till	1006-1036	22	28	24	21	2.1	7.8	7.3
	1036-1067	30	17	17	26	0.7	8.0	7.5

† Water pH – 1:1 soil/water.
‡ Salt pH = 1:1 soil/0.01*M* $CaCl_2$.

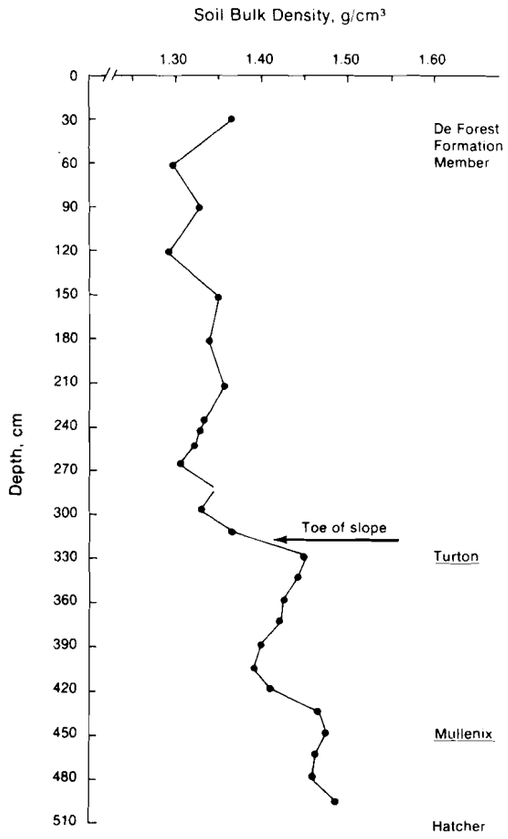

Fig. 2—Soil bulk density profile at Treynor Watershed 3, study site.

massive; friable; many strong brown (7.5YR 5/6) and brown (7.5YR 4/4) accumulations of oxides in old root channels.

Selected physical and chemical analyses (Table 1) were run on samples to a 10.7-m depth in order to establish the depth of the loess-till interface. Past literature references to the Treynor, Iowa, watersheds have assumed the loess-till interface (a slowly permeable barrier to downward water flow) to be at the gully streambed. The soil material was sectioned into the different DeForest members (Table 1) from percentage organic matter, pH values, particle-size fractions, horizon color changes, bulk density data (Fig. 2) and from the data of W. H. Allen[4] (1971) and Daniels and Jordan (1966).

Table 2—Physical properties of certain stratigraphic units within the study area (from Allen, 1971[4]).

Stratigraphic unit	2 μm Clay†	Bulk density†
	%	g/cm³
Turton	28.4	1.20
Mullenix	27.7	1.46
Hatcher	25.5	1.53
Watkins	23.3	1.53
Solum of Wisconsin Loess	26.9	1.21
Noncalcareous Wisconsin Loess	22.1	1.27
Upper Calcareous Wisconsin Loess	17.2	1.38
Lower Calcareous Wisconsin Loess	16.7	1.41
Basal Wisconsin Loess—Farmdale	22.8	1.46

† Average values among all sites for defined zones within Wisconsin Loess and average values of access tube no. 9 (tube at lowest elevation) for the post-Wisconsin alluvial fills.

The DeForest formation is predominantly silt with a reasonably uniform clay content (Table 1). Since the sediments in the alluvial deposits are composed of the particles eroded, transported, and redeposited by water action, they are similar in composition to the parent material, loess. A comparison of Tables 1 and 2 indicates the clay fraction and the soil bulk density of the alluvium are greater than that reported for the undisturbed loess.

At our site, the Turton member overlies the Mullenix at a 335 cm depth with the Mullenix-Hatcher boundary at 457 cm, and the Hatcher-Watkins boundary at 853 cm (Table 1). Vertical cleavage planes are predominant within the Turton member. Vertical and horizontal pores < 3 mm in diameter are common. As Daniels and Jordan (1966) have noted, the major difference between alluvium and loess is that the alluvium has many horizontal pores and the loess, few horizontal pores. The resulting vertical-to-horizontal saturated hydraulic conductivity ratio greatly influences the mass slumping of gully walls. The high density and lack of large pores in the Mullenix member causes abrupt changes

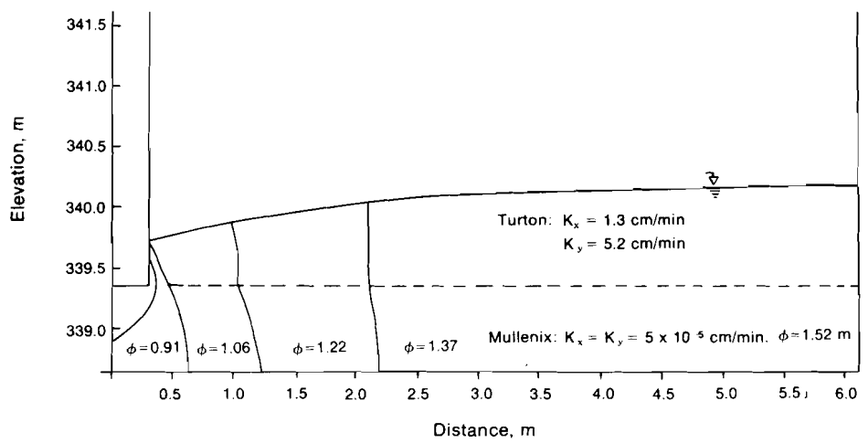

Fig. 3—Equipotential lines for discharge through the vertical gully wall at time of initial slope failure at piezometer row A. Kx, Ky, and ϕ are the horizontal saturated hydraulic conductivity, vertical saturated hydraulic conductivity, and equipotential lines, respectively.

Table 3—Relation of height of vertical slope to surface of seepage at initial slope failure and final volume of failure mass.

Location of cross section†	Height of vertical wall	Height of seepage above toe at initial failure†	Surface width of final failure mass§	Volume of failure mass§
	cm			m^3
PA	350.8	29.3	162.2	3.95
TA	318.5	29.3	154.5	3.43
PB	288.3	39.0	133.5	2.67
TB	281.3	31.1	105.8	2.03
PC	281.0	31.1	75.3	1.43

† Refer to Fig. 1, where Piezometer Row A is PA, etc.
‡ Calculated as distance from toe of the slope.
§ Volume of failure mass is measured on a unit width basis at the stage of final equilibrium.

in saturated hydraulic conductivity and shearing strength from the Turton member above.

In the side-valley watersheds in western Iowa, members of the DeForest formation cover a considerable part of the total land area, with much of the gullying in the Treynor area watersheds confined to this formation. An analysis of the geomorphology of the soil system is required for an understanding of failures in gully walls.

Ground Water Pressures and Failure Surfaces

The water level within the 3-m trench (Fig. 1) was raised by 15-cm increments. For each incremental rise in trench water surface and at a state of equilibrium for the positive pore water pressures, tensiometer and piezometer readings were recorded. The increase in pore water pressure within the soil mass ultimately resulted in slope failure. The boundaries of the failure surfaces were recorded by on-site observations, conventional photography and by overhead photography after each period of slope failure. Photographs by an aerial camera mounted 15 m above ground on a boom truck allowed compilation of large-scale topographic and cross-sectional surveys of failure sequences by photogrammetric methods.

Although four sets of tensiometers and eight sets of piezometers were read for each 15-m vertical plane, this fragmentary data is clearly inadequate for constructing an accurate flow-net for all points critical to a slope stability analysis. Recourse was, therefore, made to compute flow-nets by numerical techniques of Desai and Abel (1972), using assumptions regarding (i) the depth to impermeable barrier and (ii) the vertical-to-horizontal hydraulic conductivities. The flow-net construction will be discussed in a future report; however, the numerical technique employed the finite element methods of Desai (1972) for the steady, unconfined seepage category. Two-dimensional flow-net systems and 2-dimensional failure surfaces were plotted for vertical planes perpendicular to the initial vertical wall by extrapolating the negative pore pressures above the piezometer rows from the tensiometer readings. Table 3 shows the relation of height of vertical wall to surface of seepage at the time of initial slope failure and to volume of failure mass for the five cross sections. Figure 3 presents the equipotential lines in the vicinity of the failure mass at initial slope failure for the vertical plane through piezometer row A. The saturated conductivity for the material immediately below the toe was experimentally determined as 5×10^{-5} cm/min, whereas the material immediately above the toe was 5.2 cm/min. Figure 4 includes a plot at different equilibrium times of the piezometric head (in tube PA1) 0.2 m from the existing slope face, as a function of the piezometric head at the piezometer (PA8) near the trench (row A); Fig. 4 shows a break in the relationship between the two piezometric potential at slope failure. Figure 5 sketches to scale the series of slides at tensiometer row A. Although no undercutting at the toe of the slope was observed for the particular cross section of tensiometer row A, "popouts" of the type visualized in Fig. 6 occurred at several locations along the study wall.

In Situ Soil Strength Relations

Slope failure results if the driving forces exceed the resisting forces within the soil mass. Raising the phreatic surface within the potenial failure mass by increasing the trench water level decreases the ratio of the resisting forces to the driving forces by (i) increasing the unit weight of the soil mass, (ii) decreasing the shearing strength of the soil, and (iii) increasing the seepage forces acting parallel to the potential failure surface. Attempts were made to estimate the change in soil strength, due to a rise in phreatic surface, using a Pilcon[3] hand vane shear device. Before and immediately after the initial slope failure, shear strengths were taken along the vertical wall at tensiometer row A by removing about 15 cm of soil and inserting the 3.8-cm diameter vane 8 cm into the wall. Mean values from 7 duplicate tests at 30.5 cm vertical intervals are reported by Fig. 7. Differences in both water content and soil strength between the two samplings occurred. However, the shear strength differences are magnified because of an increase in water content after failure due not to the rise in phreatic surface but to the surface conditions of the vertical face. The amount of evaporative drying on the vertical surface before failure greatly exceeds that immediately after a large failure. Therefore, drying of the soil mass by the afternoon sun caused a part of the large differences in shear strengths between the two curves.

Stability Calculations

The stability of natural or excavated slopes is usually evaluated by either stress analysis methods or limit equilibrium methods (Skempton and Hutchinson, 1969). Stress analysis methods are based on assumed linear elastic stress-

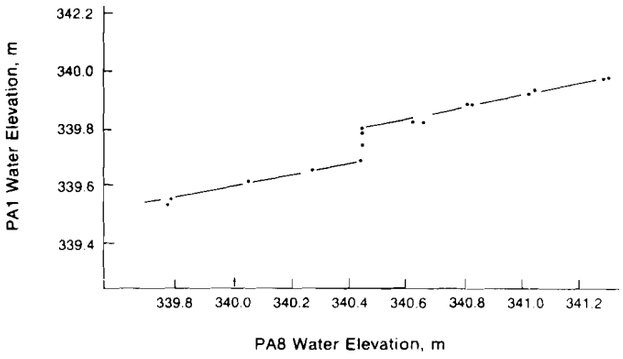

Fig. 4—Elevation of piezometric surface near vertical wall as a function of piezometric surface near trench (PA8) at different equilibrium times. The elevation of toe of vertical wall is 339.36 m above sea level.

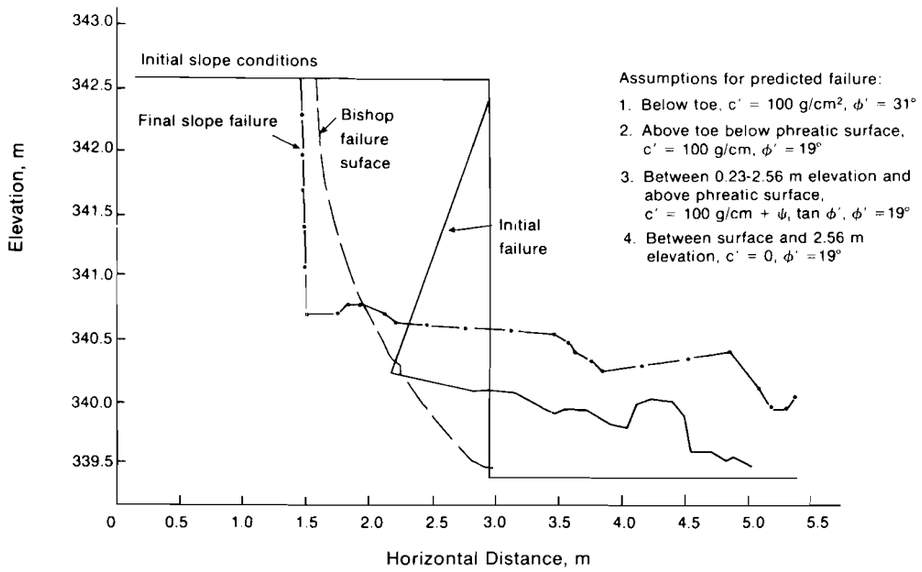

Fig. 5—Cross sectional failure surface sequence as observed at tensiometer row A and as predicted by the Bishop method of slices.

Fig. 6—Popout failure that develops at base of gully wall.

strain behavior and permit determinations of strains and stress distribution throughout the entire slope. However, equilibrium analysis methods are based on assumed plastic stress-strain behavior and permit calculations of the overall stability only on assumed sliding surfaces.

In limiting equilibrium methods, the overall stability of a sliding mass is expressed by a factor of safety, FS, which is the ratio of available resisting to actuating forces. The shear strength of soils is usually expressed by Coulomb's equation:

$$\tau_f = c' + (\sigma_n - \mu) \tan \phi'$$

where c' = the cohesion expressed in terms of effective stresses,

ϕ' = the friction angle expressed in terms of effective stresses,

σ_n = the total normal stress on the failure plane at time of failure, and,

μ = the pore water pressure.

Stability analyses were performed using the circular limit equilibrium Bishop method of slices (Bailey and Christian, 1969). In situ vane shear strength data at failure (Fig. 7) was used for an analysis of the cross section at tensiometer row A. Unit soil weights were calculated from the bulk density data of Fig. 2 and water contents for the condition of failure from Fig. 7. Assuming 2-dimensional circular-arc failure surfaces passing through the slope toe, the minimum factor of safety based on vane tests was found to be 3.36, an unrealistically high value.

To evaluate the effective stress soil parameters, a limited number of consolidated, drained triaxial compression tests were conducted on undisturbed samples intended primarily as preliminary explorations of the strength of alluvial soils. Test specimens were taken from the 320 to 335 cm depth (below the toe of the slope) and from the 274 to 290 cm depth with an 8.9-cm diameter Shelby[3] thin-walled sampler. The diameter was reduced to 7.1 cm by trimming with a rotary soil trimmer. The specimens were 15.2 cm long. Triaxial tests were carried out in a Wykeham Farrance[3] rotating bushing triaxial cell. After the specimens had been saturated and consolidated for 1 week, they were sheared at a rate of 0.005 cm/min to determine their peak strength. The corresponding effective stress shear strength parameters for the two depths are:

274–290 cm: $c' = 100$ g/cm², $\phi' = 19°$
320–335 cm: $c' = 100$ g/cm², $\phi' = 31°$.

An effective stress analysis showed that the depth of zero cohesion required for a FS of 1.0, with a friction angle of 19°, is 87 cm (Fig. 5). The measured pore water pressures were used in these calculations. Since cohesion increases

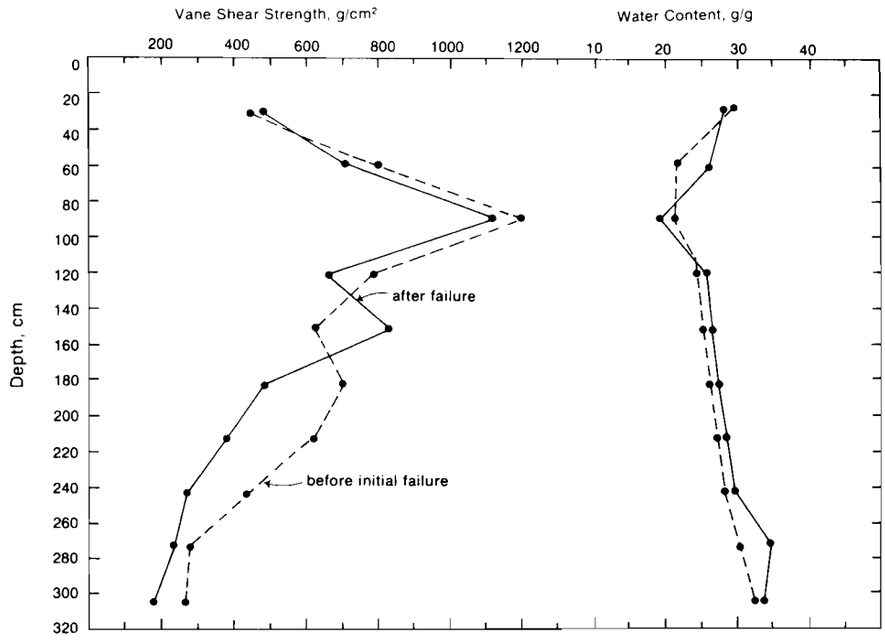

Fig. 7—Differences in vane shear strength and water content taken before and after slope failure.

with suction for loessial soils (Akiyama[6], 1964; Turnbull, 1968), c_i at any given height above the phreatic surface was calculated as equal to $c'_o + \psi_i \tan \phi'_o$, where ψ_i is the soil water suction at height i above the phreatic surface, and c'_o and ϕ'_o are the shear strength parameters for the saturated soil above the toe. The values of ψ_i were calculated from the tensiometer readings. The calculated depth of zero cohesion is not consistent with the morphological description; however, the cohesion mobilized along vertical cleavage planes at failure is difficult to determine with accuracy.

CONCLUSIONS

The major conclusions of this study are:

1) Piezometers, if carefully positioned, can be used to predict time of mass slumping of gully walls. During continuous runoff events, renewed erosion, due to sloughing of gully banks, can be described from sediment concentration-runoff curves. However, if slumping occurs but runoff is not sufficient to remove the fallen debris, the time of slumping is not known. To better understand gully erosion mechanisms, recording the time of bank failure as well as the time of its removal from the channel would be helpful. A network of continuous recording piezometers could establish time of massive slumping in relation to soil water pressure in the gully banks, to wetting and drying, and to rate of water drawdown in the gully channel.

2) Conventional limit equilibrium slope stability methods do not predict gully wall failure volumes nor do they give insights into the mechanics of the failure. As seen in Fig. 5, a single circular-arc Bishop failure surface cannot be used when the failure occurs incrementally. Stress analysis methods have been used to offer insights concerning strains and stress distributions around slopes and local failures within slopes (Dunlop and Duncan, 1970), although no analyses have been made on slopes in loessial soils having structural discontinuities and anisotropic strength conditions. Any stability analysis of slopes is limited by our ability to accurately measure soil properties within each horizon of the failure mass, but the anisotropic behavior of loess-derived alluvium and radical change in shear strength with changing moisture content makes it, in practice, impossible to describe the forces resisting failure along the entire failure surface.

3) As seen from an effective stress analysis, the vertical cleavage planes or discontinuities in the upper soil horizons result in low cohesion being mobilized along the potential failure surfaces. Zero cohesion to a depth of 87 cm was calculated from the Bishop method of slices; but, on the other hand, vertical cleavage planes were noted at the 200-cm depth, within the Turton member of the DeForest formation alluvium. The prismatic structural units and vertical cleavage planes prevent the soil from failing by an exact circular-arc type failure as seen in Fig. 5. The failure plane almost certainly follows a cleavage plane.

4) The analysis of gully bank slumping is complicated not only by the vertical cleavage planes, but also by the loss of support at the toe of the slope. The potential of loessial soil to collapse upon saturation by water has been suggested by Handy (1973) as a possible contributing factor to gullying. The loss of basal support in loess clay banks of gullies may be due to the loss of loessial soil strength upon saturation. Seepage forces appear to play a minor role in the failure processes. The key to predicting the mass of soil slumping within a gully lies in an integrated examination of the morphologic, hydrologic and soil strength relations.

LITERATURE CITED

1. Bailey, W. A., and J. T. Christian. 1969. ICES LEASE-1, A Program oriented language for slope stability analysis. R69-22, Soil Mechanics Publ. No. 235, Dep. of Civil Eng. Massachusetts Inst. of

[6]F. M. Akiyama, 1964. Shear strength properties of Western Iowa loess. M. S. Thesis. Iowa State Univ., Ames.

Tech., Cambridge, Massachusetts.

2. Brice, J. C. 1966. Erosion and deposition in the loess-mantled Great Plains, Medicine Creek drainage basin, Nebraska. Geological Surv. Prof. Pap. 352-H, p. 255–339.
3. Daniels, R. B., and R. H. Jordan. 1966. Physiographic history and the soils, entrenched stream systems, and gullies, Harrison County, Iowa. USDA Tech. Bull. 1348.
4. Desai, C. S. 1972. Finite element procedures for seepage analysis using an isoparametric element. Volume II, p. 799–824. *In* C. S. Desai (ed) Applications of the finite element methods in geotechnical engineering. U.S. Army Eng. Waterw. Exp. Stn., Corps of Engineers, Vicksburg, Mississippi.
5. Desai, C. S., and J. F. Abel. 1972. Introduction to the finite element method. Van Nostrand Reinhold Company, New York. 477 p.
6. Dunlop, P., and J. M. Duncan. 1970. Development of failure around excavated slopes. J. Soil Mech. Found. Div., Proc. Am. Soc. Civil Eng. 96:471–493.
7. Handy, R. J. 1973. Collapsible loess in Iowa. Soil Sci. Soc. Am. Proc. 37:281–284.
8. Piest, R. F., J. M. Bradford, and R. G. Spomer. 1975. Mechanisms of erosion and sediment movement from gullies. p. 162–176 *In* Present and prospective technology for predicing sediment yields and sources. ARS-S-40. ARS-USDA
9. Piest, R. F., and R. G. Spomer. 1968. Sheet and gully erosion in the Missouri Valley loessial region. Trans ASAE 11(6):850–853.
10. Ruhe, R. V., R. B. Daniels and J. G. Cady. 1967. Landscape evolution and soil formation in southwestern Iowa. USDA Tech. Bull. 1349.
11. Saxton, K. E., and R. G. Spomer. 1968. Effects of conservation on the hydrology of loessial watersheds. Trans ASAE 11(6):348–349.
12. Skempton, A. W., and J. Hutchinson. 1969. Stability of natural slopes and embankment foundations. 7th Int. Conf. Soil Mechanics and Foundation Engineering, State-of-the-Art Volume, pp. 291–340.
13. Turnbull, W. J. 1968. Construction problems experienced with loess soils. Highway Research Record No. 212, Conference on loess: Design and Construction, p. 12.